

See discussions, stats, and author profiles for this publication at: <https://www.researchgate.net/publication/263945517>

Bacterial Attachment and Viscoelasticity: Physicochemical and Motility Effects Analyzed Using Quartz Crystal Microbalance with Dissipation (QCM-D)

ARTICLE in ENVIRONMENTAL SCIENCE & TECHNOLOGY · DECEMBER 2012

Impact Factor: 5.33 · DOI: 10.1021/es303394w

CITATIONS

15

READS

95

4 AUTHORS:



Jenia Gutman

Ministry of Agriculture & Rural Development, I...

9 PUBLICATIONS 108 CITATIONS

SEE PROFILE



Sharon L Walker

University of California, Riverside

103 PUBLICATIONS 2,849 CITATIONS

SEE PROFILE



Viatcheslav Freger

Technion - Israel Institute of Technology

77 PUBLICATIONS 2,092 CITATIONS

SEE PROFILE



Moshe Herzberg

Ben-Gurion University of the Negev

54 PUBLICATIONS 1,669 CITATIONS

SEE PROFILE

Bacterial Attachment and Viscoelasticity: Physicochemical and Motility Effects Analyzed Using Quartz Crystal Microbalance with Dissipation (QCM-D)

Jenia Gutman,[†] Sharon L. Walker,[‡] Viatcheslav Freger,[§] and Moshe Herzberg^{*,†}

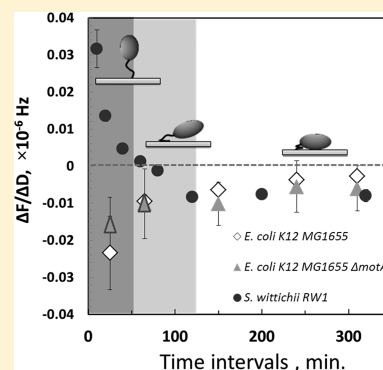
[†]Department of Desalination and Water Treatment, Zuckerberg Institute for Water Research, Albert Katz International School for Desert Studies, Jacob Blaustein Institute for Desert Research, Ben Gurion University of the Negev, Israel 84990

[‡]Department of Chemical and Environmental Engineering, University of California, Riverside, California 92521, United States

[§]The Wolfson Department of Chemical Engineering, Technion - Israel Institute of Technology, Haifa 32000, Israel

Supporting Information

ABSTRACT: This investigation is focused on the combined effect of bacterial physicochemical characteristics and motility on cell adhesion and deposition using a flow-through quartz crystal microbalance with dissipation (QCM-D). Three model flagellated strains with different degrees of motility were selected, including a highly motile *Escherichia coli* K12 MG1655, an environmental strain *Sphingomonas wittichii* RW1, and a nonmotile (with paralyzed flagella) *Escherichia coli* K12 MG1655 Δ *motA* that is incapable of encoding the motor torque generator for flagellar movement. Of the three strains, *S. wittichii* RW1 is highly hydrophobic, while *E. coli* strains are equally hydrophilic. Consideration of the hydrophobicity provides an alternative explanation for the bacterial adhesion behavior. QCM-D results show that motility is a critical factor in determining bacterial adhesion, as long as the aquatic chemical conditions are conducive for motility and the substratum and bacterial surface are similarly hydrophobic or hydrophilic. Once their properties are not similar, the contribution of hydrophobic interactions becomes more pronounced. QCM-D results suggest that during adhesion of the hydrophobic bacterium, *S. wittichii* RW1, the initial step of adhesion and maturation of bacteria–substratum interaction on hydrophilic surface includes a dynamic change of the viscoelastic properties of the bond bacterium–surface becoming more viscously oriented.



1. INTRODUCTION

Biofilm formation is a well-known environmental phenomenon. It represents an ancient, protected mode of growth that allows microbial survival in hostile environments and allows microorganisms to disperse and colonize new niches.¹ This sophisticated bacterial life form is widely found on ship hulls, power plant piping, water supply, irrigation systems, and many other locations.^{2–4} In some cases biofilm development is beneficial and hence encouraged, such as in biological wastewater and water treatment processes;^{5–8} however, in the majority of the cases it is undesired and causes increased consumption of energy and chemicals, inefficient operation, and shutdown of the impacted system. Recently, another niche, where biofilms prove particularly detrimental, has caught practitioners' and researchers' attention, namely, the nanofiltration (NF) and reverse-osmosis (RO) membrane processes used for wastewater treatment. Microbial biofilms on RO membranes inflict considerable damage to RO system performance, exacerbated by the fact that the system does not allow for backwash or disinfection with oxidative agents.⁹ Since the commercially available RO desalination units experience biofouling problems, widespread application of this technology for complete reclamation of wastewater is limited.⁴

A preliminary step in the biofilm formation process is bacterial deposition and attachment.^{4,10} Recently, these two stages have been linked to flagellar presence and activity.¹¹ Wood et al.¹² demonstrated that the best biofilm forming bacterial strains displayed the highest motility, while strains least prone to forming biofilms were motility-impaired. Surface coverage and complexity of the biofilm structure were also related to motility and presence of flagella.¹² Influence of flagella on initial bacterial attachment was related to various parameters including, among others, time of interaction with the surface,¹¹ ionic strength,¹³ growth phase, and presence of divalent cations.^{14–17} de Kerchove and Elimelech¹⁴ demonstrated that adhesion of motile cells was mostly governed by the steric and electrostatic interactions between the flagella and the surfaces.^{14,18} In conclusion, the contribution of flagella to bacterial adhesion is based on two possible mechanisms: (1) involvement of flagella in the physical attachment to surfaces, overcoming repulsive forces at the surface–medium interface,

Received: August 21, 2012

Revised: November 25, 2012

Accepted: November 27, 2012

Published: November 27, 2012

which promotes adherence and facilitates irreversible adhesion; and (2) flagella-induced spreading of the bacteria on abiotic surfaces.^{12,19}

The contribution of flagella to biofilm architecture was previously investigated using a number of flow regimes and relevant bacteria.^{11,12,14,20} Of these, the use of tangential flow cells in quartz crystal microbalance with dissipation (QCM-D) has been successfully demonstrated as an adequate and accurate technique for characterization of fouling and biofilm formation processes.^{21,22} QCM-D is an acoustic method which records the amount and assesses the viscoelastic properties of an adhering mass as changes in the resonance frequency (Δf) and energy dissipation (ΔD). Plotting the change in dissipation versus the change in frequency makes it possible to compare the induced energy dissipation per coupled unit mass. A lower $\Delta f/\Delta D$ value indicates buildup of a dissipative soft and fluid film on the QCM-D sensor. On the other hand, a high $\Delta f/\Delta D$ value stands for a more rigid layer.^{22–24} This information may thus help elucidate the biofilm structure and conformation. For instance, an increase in the bacterial layer rigidity was suggested to be a sign of progressive and maturing cell attachment.^{22,25,26} Thus, the degree in frequency and dissipation changes of the QCM-D sensor and the effects of loosely bound layers of bacteria can be used to analyze bacteria–substratum interactions. Careful interpretation of the frequency shift acquired during bacterial deposition on the QCM-D sensor should be taken into account as the frequency and dissipation response was suggested to be influenced by cell surface morphology with some cases, where frequency shift increased with the increase of bacterial adhesion.^{27,29} The most common explanation for this phenomenon is based on the coupled oscillator theory that describes the connection of bacteria or micrometer-sized particles as an elastic spring-like connection²⁷ to the sensor surface. This elastic connection can counterbalance the added inertia by the attached bacteria and lead to positive frequency shifts. Therefore, QCM-D can be used to quantify bacterial attachment rate only if frequency shift results are supported by direct microscopy.^{28,29} Monitoring resonance frequency and dissipation can be used to obtain viscoelastic and inertial characteristics of the deposited layers.^{30,31} Furthermore, acquiring several overtone frequencies is another advantageous feature of QCM-D, since elastic, inertial, and dissipative viscous contributions to frequency and dissipation shifts depend on frequency in a different manner. Thus, the evolution of the bond between bacteria and the surface as well as its viscoelastic properties can be delineated with QCM-D analysis.

A model microorganism, which is relevant to biofilms in RO wastewater treatment, was selected for this study and compared to well characterized motile and nonmotile *E. coli* strains. It was previously reported that members of the genus *Sphingomonas* were found to initiate and dominate biofilms on RO membranes in installations used for treatment of tertiary municipal wastewater.^{32–34} A representative of this genus, *Sphingomonas wittichii* RW1, was chosen as a model strain to study the attachment and evolution of the bacterial layer. In fact, *Sphingomonas* members widely occur in the environment, which can be related to their ability to metabolize large varieties of organic compounds and even to proliferate under oligotrophic conditions.³⁵ As already mentioned, in addition to *Sphingomonas wittichii*, *Escherichia coli* K12 MG1655 and nonmotile flagellated *E. coli* K12 MG1655 $\Delta motA$ ³⁶ strains were selected. The motility and physicochemical properties of the selected model strains were examined in the context of

initial adhesion to the surface and the viscoelastic properties of bacteria–surface contact using QCM-D.

2. MATERIALS AND METHODS

2.1. Model Bacterial Strain and Media. *Sphingomonas wittichii* RW1 (GenBank #NC 00951) was obtained from the DSMZ (Deutsche Sammlung von Mikroorganismen und Zellkulturen GmbH) culture collection, Germany. The bacterium was grown on nutrient agar medium containing peptone (5 g/L) and meat extract (3 g/L) adjusted to pH 7 and supplemented with 200 $\mu\text{g/mL}$ streptomycin (Sigma Aldrich, S6501).²⁷ *E. coli* strains K12 MG1655 and K12 MG1655 $\Delta motA$ (obtained from the *E. coli* genome project, University of Wisconsin, Madison) were grown on Luria–Bertani (LB) medium.³⁷

Bacterial cultures were grown from a single colony by incubation at 150 rpm and 30 °C. The cells were diluted in a nutrient broth medium (1:100) and analyzed at their early stationary phase (8 h for *E. coli* and 24 h for *S. wittichii*). Bacteria were harvested by centrifugation (4000g and 4 °C for 10 min) and washed three times with NaCl solution at the same ionic strength (IS) as the subsequent experiment. After harvesting and washing the bacteria, the optical density (OD_{600}) of the suspension was adjusted to 1 for all subsequent experiments and corresponded to $5 \times 10^8 \pm 5 \times 10^6$ cells/mL (unless mentioned otherwise).

2.2. Electrophoretic Mobility. The effect of ionic strength (IS) on the electrophoretic mobility of *S. wittichii* was measured by a zeta potential analyzer (ZetaPlus 1994, Brookhaven Instruments Co., Holtsville, NY). The cells were harvested, washed, and analyzed in solutions of different ionic strength (10, 30, and 100 mM NaCl). At an $\text{OD} = 1$ and 25 °C, each sample was analyzed for 2 cycles and 5 repetitions. Three repetitions were done for each IS.

2.3. Bacterial Hydrophobicity. The MATH (microbial adherence to hydrocarbons) method has been described in detail previously.³⁸ Briefly, this method is based on the cell partitioning between water and a nonpolar solvent. Suspensions (4 mL) of bacteria after washing in the relevant background solution were adjusted to a corresponding value (optical density at 600 nm of 0.3 in NaCl solution at selected IS) and transferred into test tubes containing 1 mL of the hydrocarbon (*n*-dodecane; analytical grade, Fischer scientific). The test tubes were vortexed (Vortex Genie 2, Scientific Industries, Bohemia, NY) for 2 min, followed by a 45-min rest period to allow for phase separation. The optical density of the cells in the aqueous phase was measured at 600 nm (Lambda EZ 201 model, Perkin-Elmer, Waltham, MA) to determine the extent of bacterial cell partitioning between the *n*-dodecane and the electrolyte solution. Hydrophobicities are reported as the percentages of total cells partitioned into the hydrocarbon.

2.4. Motility Assay. Motility assays were performed following a standard protocol.³⁹ Briefly, Petri dishes (diameter 85 mm) containing fresh soft agar (1% peptone and 0.3% agar [wt/vol]) with different ionic strengths of 10, 100, and 300 mM NaCl, were pinched in the center by a sterile toothpick that had been previously immersed in 24- and 8-h-old bacterial cultures of *S. wittichii* and *E. coli*, respectively. The motility agar plates were incubated in 30 °C (*S. wittichii*) or 37 °C (*E. coli*). Each test was repeated three times. Motility is represented as percent of coverage of the Petri dish by the motility halos: % coverage = $R_h/R_p \times 100$ when R_h is the halo radius, in cm, and R_p is equal to the radius for the Petri dish being used. Motility halos were

Table 1. Characterization of *E. coli* K12 MG1655 and *S. wittichii* RW1 Cells As a Function of the Ionic Strength

	ionic strength (mM)	live cells ^a	cell radius (μm) ^b	MATH results (%) ^c	electrophoretic mobility ($\mu\text{m/s}$)(cm/V) ^d
<i>E. coli</i> MG1655	10	94	1.24	5 \pm 3	-3.29 \pm 0.11
	100	92		5 \pm 4	-2.4 \pm 0.26
	300	86		11 \pm 4	-1.41 \pm 0.07
<i>E. coli</i> MG1655 ΔmotA	10	93	1.11	1 \pm 1.2	-3.69 \pm 0.18
	100	85		6 \pm 1	-2.33 \pm 0.33
	300	81		9 \pm 3	-1.09 \pm 0.34
<i>S. wittichii</i> RW1	10	96	1.04	87 \pm 5	-0.523 \pm 0.16
	100	91		88 \pm 0.2	-0.416 \pm 0.21
	300	92		83 \pm 4.8	-0.47 \pm 0.21

^aPercentage of the live cells in the population determined based on Live/Dead BacLight kit results. ^bSpherical radius calculated from the lengths and widths of individual cells (ellipse area = π ·width·length, radii of a circle = ((ellipse area)/ π)^{1/2}). The average lengths and widths of the cells were 1.76 \pm 0.125 and 0.875 \pm 0.06 μm , respectively, for *E. coli* K12 MG1655 cells, 1.58 \pm 0.06 and 0.78 \pm 0.05 for *E. coli* K12 MG1655 ΔmotA , and 1.41 \pm 0.08 and 0.77 \pm 0.03 μm for *S. wittichii* RW1. ^cMicrobial adhesion to hydrocarbons (MATH) indicates the relative hydrophobicity of the cell as the percentage of cells partitioned into *n*-dodecane versus the electrolyte solution (NaCl). ^dExperiments were conducted at ambient pH of 5.7 \pm 0.1 and temperature of 25 $^{\circ}\text{C}$. Error bars indicate one standard deviation.

measured after 18 and 40 h for the *S. wittichii* strain and 18 h for the *E. coli* strain, as *E. coli* is more motile than *S. wittichii* and motility halo expanded to the edge of the plate after more than 20 h.

2.5. QCM-D Measurement of Adhesion and Bacterial Layer Viscoelasticity. QCM-D (Q-sense AB, Gothenburg, Sweden), which employs an ultrasensitive coin-shaped quartz mass sensor housed inside a flow cell with a well-defined geometry and hydrodynamic characteristics, was used for adhesion and fluidity assays.²⁸ The QCM-D measurements were performed with AT-cut quartz crystals mounted in an E1 system (Q-sense AB, Gothenburg, Sweden). The crystals, with a fundamental resonant frequency of around 5 MHz, were coated with the amorphous silica by vapor deposition (QXS-303, Q-sense AB, Gothenburg, Sweden). All QCM-D experiments were performed under flow-through conditions using a digital peristaltic pump (IsmaTec Peristaltic Pump, IDEX) operating in pushing mode of the studied solutions that were injected to the sensor crystal chamber at 150 $\mu\text{L}/\text{min}$. For the adhesion experiments, different solutions were injected sequentially for 20 min to the QCM-D system in the following order: (i) NaCl background solutions of 10, 100, or 300 mM ionic strength; (ii) suspended bacteria in the background solution at OD = 0.1; (iii) the same background solution without bacteria. The variations of the changes in frequency (Δf , Hz) and dissipation factor (ΔD) were measured for six different overtones, $n = 3, 5, 7, 9, 11$, and 13. For characterizing the bacterial layer viscoelastic properties, the following sequence was applied: (i) 20 min injection of 100 mM NaCl background solution; (ii) 6 h injection of suspended bacteria at OD₆₀₀ of 0.1 \pm 0.01 ($5 \times 10^7 \pm 5 \times 10^6$ cells·mL⁻¹).

3. RESULTS AND DISCUSSION

3.1. Physico-Chemical Properties of Bacterial Strains.

Data presented in Table 1 display the physicochemical characteristics of the *E. coli* and *S. wittichii* strains. Electrophoretic mobility of *S. wittichii* RW1 was constant across the range of IS, whereas it decreased significantly with IS for both *E. coli* K12 strains. The latter result can be explained by decreased thickness of the electrical double layer (EDL) and decreased effective surface charge at elevated ionic strength (Table 1). However, the electrophoretic mobility of *S. wittichii* does not agree with this model.^{40,41} Since most colloids in aquatic environment are negatively charged⁴² they would be

repelled from negatively charged surfaces and at higher ionic strength the particles would be less negatively charged due to compression of the EDL by counterions, such as Na⁺ and reduction of the Stern potential.⁴³ A possible explanation for this deviation is that *Sphingomonas* differ from other gram-negative bacteria by having unusual membrane structure that does not contain lipopolysaccharides (LPS), but contains glycosphingolipids (GSL)⁴⁴ with the carbohydrate portions directed outward.⁴⁵ In a previous study, the surface charge densities of GSL were compared to LPS bilayers (as exist in *E. coli* outer membranes) and the results showed a dramatic difference. The surface charge of GSL analyzed in 50 mM KCl and 5 mM MgCl₂ supplemented with 5 mM HEPES at pH 7.4 was only 1.35 elementary charges/nm², as compared to 3.33 elementary charges/nm² for LPS.⁴⁶ In the light of the results presented in Table 1 and the previous study of Wiese et al.,⁴⁶ *S. wittichii*'s outer layer is less negative than that of *E. coli* and therefore, the ionic strength of the solution may have only a small effect on its surface potential and electrophoretic mobility.

The cell hydrophobicity, which correlates with the polarity of the surface functional groups exposed at the outer surface of the bacterial cell wall, was assessed using the MATH technique. The partitioning of approximately 83–87% into the *n*-dodecane phase for *S. wittichii*, as compared to 1–11% partitioning for both *E. coli* strains, was independent of ionic strength. This suggests that *S. wittichii* cells are dramatically more hydrophobic at all ionic strengths than the *E. coli* strains that are highly hydrophilic.

3.2. Effect of Ionic Strength on Bacterial Motility. *E. coli* K12 MG1655 was found to be significantly more motile than *S. wittichii* RW1 (Figure 1). Both of the strains exhibit optimal motility at 100 mM NaCl. This occurrence of an optimum might be explained by assuming that conditions closest to the physiological saline conditions (0.9% NaCl or about 150 mM) used in this protocol are the most favorable for flagellar rotation.¹³ A similar trend of swimming motility enhancement at 100 mM KCl was reported for *Pseudomonas aeruginosa* PAO1.¹⁸ Nonmotile *E. coli* strain exhibited no detectable motility on the soft-agar plates regardless of the ionic strength.

3.3. Bacterial Adhesion to the QCM-D Sensor. Primarily, in order to show correlation between frequency shifts and number of adhered bacteria, microscopic quantifica-

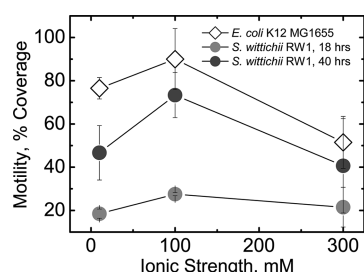


Figure 1. Effect of ionic strength, adjusted with NaCl, on the swimming motility of *S. wittichii* RW1 and *E. coli* K12 MG1655 strains after 18 h (*E. coli* and *S. wittichii*) and 40 h (only for *S. wittichii* as *E. coli* 40 h halo is bigger than the dish diameter). The area of the motility halo was calculated as a percentage out of the total area of the Petri dish.

tion of all bacterial strains attached to QCM-D surface was performed both at 100 and 300 mM (Figure 2B and C). In

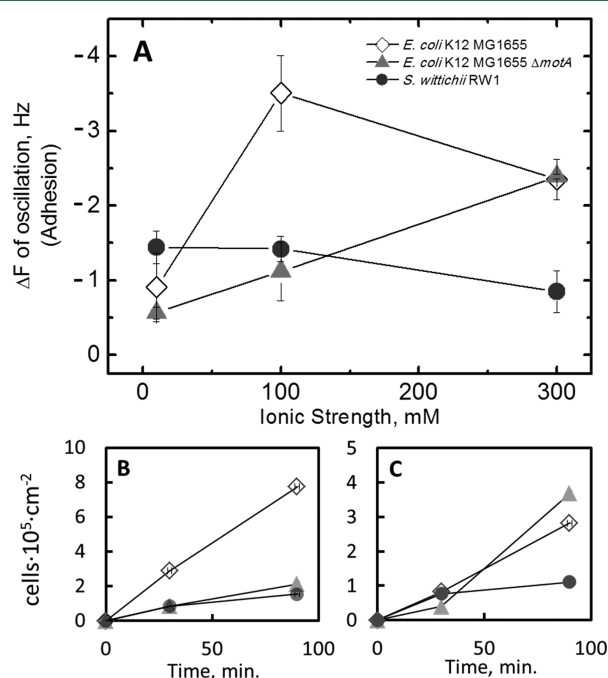


Figure 2. Effect of ionic strength, adjusted with NaCl, on the adhesion of *E. coli* K12 MG1655 and *S. wittichii* RW1 strains to silica-coated QCM-D sensor as measured both by the change in the oscillation frequency (A) and by fluorescent microscopy. Data represent average of 3–5 independent bacterial deposition measurements. QCM-D sensors were stained with DAPI, visualized, and counted at the end of the adhesion experiment being carried out at IS of 100 mM (B) and 300 mM (C).

addition, since a positive correlation between cell deposition degree and cell concentration in the feed bacterial suspension was shown by others,¹¹ a dose–response experiment, testing the effect of cell concentration on frequency shift of the sensor was carried out for all bacterial strains used in this study. Clearly, higher cell concentration results in a more pronounced frequency shift (Supporting Information, Figure S1). From the above, we can conclude there is a positive relation between frequency shifts obtained by the QCM-D and number of adhered bacteria to its sensor: Both effects of ionic strength and bacterial strain on bacterial deposition are confirmed (Figure 2B and C and Figure S1). Therefore, in this study, the mass of

attached cells can be deduced from the changes in the oscillation frequency of the QCM-D sensor (Δf , Hz).

In the QCM-D adhesion experiments with silica coated sensor, motile *E. coli* MG1655 showed the greatest change in frequency over time at 100 mM NaCl, indicative of the rate of cell deposition on the sensor. For *E. coli* K12 MG1655, the decrease in frequency at 100 mM, 3.5 ± 0.3 Hz, was higher compared to that at 10 mM, 0.91 ± 0.26 Hz (Figure 2). For *S. wittichii*, a slight increase in frequency change with decreasing ionic strength was observed, from 0.85 ± 0.14 Hz for 300 mM compared to 1.42 ± 0.1 and 1.44 ± 0.13 Hz for 100 and 10 mM NaCl, respectively. It is seen that the adhesion of *S. wittichii*, a semimotile strain, to the sensor surface at 10 and 100 mM (physiological), is nearly constant and larger at 10 mM than the adhesion of nonmotile *E. coli* strain. On the other hand, at IS of 300 mM, *S. wittichii* exhibits a change in frequency 0.85 ± 0.14 Hz that is significantly lower than both motile and nonmotile *E. coli* strains, which exhibited a frequency decrease of 2.35 ± 0.16 and 2.39 ± 0.02 Hz, respectively.

No relation between frequency change pattern (Figure 2) of the motile *E. coli* MG1655 strain and the mode of its motility could be obtained, except for 100 mM (physiological) where both motility and frequency shift were the highest. On the other hand, at high IS of 300 mM, the motility is significantly reduced from 90 ± 7 to $52 \pm 6.5\%$ coverage, for 100 and 300 mM NaCl, respectively. Therefore, we suggest that the compression of the EDL cannot solely affect adhesion that is more strongly influenced, in this case, by cell motility. The hydrophilicity of both types of *E. coli* MG1655 does not seem to affect their adhesion. It seems that when bacterial motility is paralyzed, adhesion pattern follows DLVO trend, where bacterial adhesion increases with ionic strength. Hence, the frequency change of the nonmotile *E. coli* MG1655 $\Delta motA$ is more pronounced as ionic strength is elevated. Notably, adhesion of the nonmotile *E. coli* MG1655 $\Delta motA$ is influenced solely by the compression of the EDL throughout the different ionic strengths tested; the higher the ionic strength, the higher is the change in frequency. Thus, the mode of attachment can be predicted from the electrophoretic mobility results for this strain. In the case of *S. wittichii* adhesion, electrophoretic mobility has virtually no change during the experimental conditions being studied and therefore we cannot predict any relation with cell attachment. Also *S. wittichii* swimming motility does not seem to affect its adhesion.

3.4. Viscoelastic Properties of Bacteria–Surface Bond.

The ratio $\Delta f/\Delta D$ shown in Figure 3 was established to represent the viscoelasticity of the bacterial layer formed on the QCM-D sensor, i.e. its viscous or elastic nature.^{23,31} Values of $\Delta f/\Delta D$ above 0 correspond to a positive $\Delta f/\Delta D$ slope for specific time period, which stands for higher elasticity of the layer, and negative values of $\Delta f/\Delta D$ slope stand for a more viscous layer.²⁹ Figure 3 provides a thorough look into the bacterial layer behavior during the very initial stage of bacterial adhesion (first 20 min of bacterial injection) as well as during the last hour (sixth) of the experiment. Since increasing overtone number results in higher frequency of the sensor, comparison of results through the applied overtone range provides a stronger evidence for the hypothesized bacterial adhesion mode. As it appears from Figure 3, the only strain whose adhesion is dynamic in the sense of its viscoelasticity is *S. wittichii* during its initial stages of adhesion. As expected, the

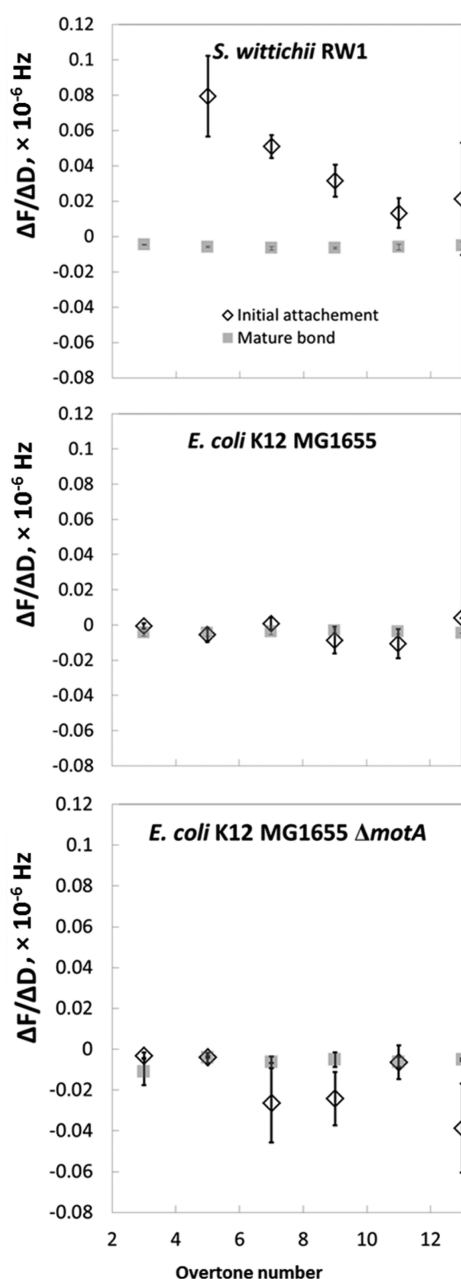


Figure 3. Slopes of the frequency vs dissipation shifts, ($\Delta f/\Delta D$), during first 20 min of the experiment (initial attachment) and during the last, 6th hour of bacterial deposition (mature surface–bacteria bond) on the QCM-D sensor, as a function of the overtone number for each bacterial strain. Data represent average of 3–5 independent bacterial deposition measurements at IS of 100 mM adjusted with NaCl.

viscoelastic characteristics of the bacteria–substrate bond change toward more viscous as the overtone number increases.

In Figure 4, the instantaneous values of the slope, $\Delta f/\Delta D$ for the 20–100 min range of the experiment provide a dynamic picture of the viscoelastic changes over time course of 6 h for the layer of *S. wittichii*. These values are compared to ones of the *E. coli* strains' layers. While for the layers of *E. coli* strains, viscoelasticity remains relatively steady (comparing to *E. coli*) throughout the whole deposition experiment, suggesting a more steadily viscous layer. In the case of *S. wittichii*, the viscoelasticity of the bacterial layer is dynamic, characterized by

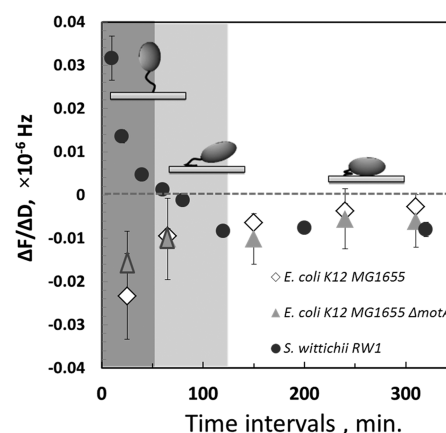


Figure 4. Slopes of the frequency vs dissipation shifts, ($\Delta f/\Delta D$) during the entire 6 h period of the bacterial deposition experiment. Average slopes represent periods of 20–100 min during the 6 h deposition experiment with the QCM-D flowcell. The middle time point of each period is plotted against the slope of $\Delta f/\Delta D$ for the 9th overtone. Inset image illustrates the suggested process of bond maturation and the consequent more viscous bacterial layer of *S. wittichii* attached to the sensor surface through time. Data represent average of 3–5 independent bacterial deposition measurements at IS of 100 mM adjusted with NaCl.

elastic properties during initial stages of attachment (first 50 min of the experiment, dark gray area in Figure 4). Between the first and the second hour of the experiment, a stabilization of the viscoelastic properties was observed, as the bacterial layer became viscous (values below 0, light gray area in Figure 4). Through the rest of the experiment (additional 4 h, white area Figure 4) *S. wittichii* layer viscoelastic properties remained constantly viscous.

The observation that the motility (in the case of *E. coli* strains) has almost no effect on the bacterial layer viscoelasticity (Figure 3) might be explained by the fact that bacteria lose their motility once adhered to a surface. It was suggested previously that flagellar activity contributes to bringing the cells in close proximity to the surface⁴⁷ but this activity ceases once the cell is attached.^{48–50} Gibiansky et al.⁵¹ found that flagellar activity is unnecessary for the cell positioning on its target site on the surface. In that case, the physicochemical characteristics of the motile and nonmotile *E. coli* strains are similar, and therefore, the viscoelastic properties of their layer are likely identical. For the elasticity of the *S. wittichii* layer, the results can be explained by a possible effect of the cellular hydrophobicity/hydrophilicity on the bacterial layer viscoelasticity and a dynamic nature of the bacterial layer's mechanical characteristics. It can be hypothesized that *S. wittichii* structure, in which a single flagella is attached to a highly hydrophobic, nearly neutrally charged body, provides a composite combination between two distinct physicochemical units. While the proteinaceous⁵² flagella of *S. wittichii* are hydrophilic and charged⁵³ and readily attach to the silica surface, its hydrophobic body, which is repelled from the surface, remains at a certain distance from the sensor surface. We have shown in our lab that this form of bacterial attachment results in a highly elastic substratum–bacteria bond on the sensor's surface.²⁹ Interestingly, the model of bond maturation suggested recently by Olsson²³ proposes explanation for the dramatically declining elasticity as a result of bond maturation and narrowing gap between the hydrophilic surface and the hydrophobic bacterial body. Here we suggest

two subsequent steps in bacterial adhesion to surfaces: initial attachment of polar flagellar end of the cell followed by water release from the bacteria–surface interface and bond maturation, as suggested by previous studies.^{23,53}

In conclusion, motility is an important factor for determining the mode of bacterial adhesion, as long as the aquatic chemical conditions are physiologically conducive for motility and the surface and the bacteria are of a similar hydrophobicity/hydrophilicity. Under other conditions, physicochemical properties are presumed to determine the fate of bacterial adhesion. For the *Sphingomonas* genus the exceptional hydrophobicity and stable, nearly neutral surface charge might be a partial explanation for its ability of pioneering colonization and dominance in RO systems desalinating wastewater effluents.^{26,34} Given sufficient time, this strain is capable of spreading over vast areas. The viscoelastic properties of the surface–bacterium bond influencing the bacterial layer is suggested to be affected by the hydrophobicity/hydrophilicity of the bacterial strain. We propose that for the hydrophobic *S. wittichii*, the initial bond maturation is an energy demanding and kinetically limiting step that probably involves a release of water and closure of the gap between the bacteria and surface.⁵⁴ While this supposition of water release has already been suggested in various studies, further confirmation of this hypothesis using QCM-D and other interfacial techniques is needed. In the context of *Sphingomonas* strains being the ones to initiate and dominate the biofilms on RO membranes, increasing the wettability and swelling of the membrane–water interface might assist in preventing bacterial attachment and subsequent biofilm development.²⁷ Future research on the properties of extracellular polymeric substances (EPS) of this species, as well as its oligotrophic characteristics, will also allow better understanding of biofilm establishment in RO environments.

■ ASSOCIATED CONTENT

● Supporting Information

Figure S1, Frequency shift of the QCM-D sensor as a function of cell concentration in the feed bacterial suspension injected into the QCM-D flow-cell. This material is available free of charge via the Internet at <http://pubs.acs.org>.

■ AUTHOR INFORMATION

Corresponding Author

*Tel: 972-8-6563520; fax: 972-8-6563503; e-mail: herzberg@bgu.ac.il.

Notes

The authors declare no competing financial interest.

■ ACKNOWLEDGMENTS

This research was supported by the following funds: Israel Science Foundation (grant No. 1360/10), J. Gutman's Ph.D. fellowship provided by the Israeli Water Authority and S. L. Walker was supported by the U.S. Fulbright Program during sabbatical at the Zuckerberg Institute for Water Research in Ben Gurion University.

■ REFERENCES

- (1) Hall-Stoodley, L.; Costerton, J. W.; Stoodley, P. Bacterial biofilms: From the natural environment to infectious diseases. *Nat. Rev. Microbiol.* **2004**, *2*, 95–108.
- (2) Davey, M. E.; O'toole, G. A. Microbial biofilms: From ecology to molecular genetics. *Microbiol. Mol. Biol. Rev.* **2000**, *64*, 847–867.

- (3) Dunne, W. M., Jr. Bacterial adhesion: Seen any good biofilms lately? *Clin. Microbiol. Rev.* **2002**, *15*, 155–166.
- (4) Flemming, H. C. Biofouling in water systems—Cases, causes and countermeasures. *Appl. Microbiol. Biotechnol.* **2002**, *59*, 629–640.
- (5) Gujer, W. Nitrification and me-A subjective review. *Water Res.* **2010**, *44*, 1–19.
- (6) Thompson, J.; Lin, N.; Lyster, E.; Arbel, R.; Knoell, T.; Gilron, J.; Cohen, Y. RO membrane mineral scaling in the presence of a biofilm. *J. Membr. Sci.* **2012**, *415–416*, 181–191.
- (7) Herzberg, M.; Dosoretz, C. G.; Tarre, S.; Michael, B.; Dror, M.; Green, M. Simultaneous removal of atrazine and nitrate using a biological granulated activated carbon (BGAC) reactor. *J. Chem. Technol. Biotechnol.* **2004**, *79*, 626–631.
- (8) Herzberg, M.; Dosoretz, C. G.; Tarre, S.; Belavski, M.; Green, M.; van Loosdrecht, M. Biological granulated activated carbon fluidized bed reactor for atrazine remediation. *Water Sci. Technol.* **2004**, *49*, 215–222.
- (9) Ridgway, H. F. National Water Research Institute Occasional Paper NWRI-97-3. Membrane Biofouling: An International Workshop, Sydney, Australia, 1997; pp 75–79.
- (10) Goulter, R.; Gentle, I.; Dykes, G. Issues in determining factors influencing bacterial attachment: a review using the attachment of *Escherichia coli* to abiotic surfaces as an example. *Lett. Appl. Microbiol.* **2009**, *49*, 1–7.
- (11) Haznedaroglu, B. Z.; Zorlu, O.; Hill, J. E.; Walker, S. L. Identifying the role of flagella in the transport of motile and nonmotile *Salmonella enterica* serovars. *Environ. Sci. Technol.* **2010**, *44*, 4184–4190.
- (12) Wood, T. K.; González Barrios, A. F.; Herzberg, M.; Lee, J. Motility influences biofilm architecture in *Escherichia coli*. *Appl. Microbiol. Biotechnol.* **2006**, *72*, 361–367.
- (13) Berg, H.; Lindh, L.; Arnebrant, T. Intraoral lubrication of PRP-1, statherin and mucin as studied by AFM. *Biofouling* **2004**, *20*, 65–70.
- (14) de Kerchove, A. J.; Elimelech, M. Calcium and magnesium cations enhance the adhesion of motile and nonmotile *Pseudomonas aeruginosa* on alginate films. *Langmuir* **2008**, *24*, 3392–3399.
- (15) Houry, A.; Briandet, R.; Aymerich, S.; Gohar, M. Involvement of motility and flagella in *Bacillus cereus* biofilm formation. *Microbiology* **2010**, *156*, 1009–1018.
- (16) Marshall, K. C.; Stout, R.; Mitchell, R. Mechanism of the initial events in the sorption of marine bacteria to surfaces. *J. Gen. Microbiol.* **1971**, *68*, 337–348.
- (17) Khan, S. Rotary chemiosmotic machines. *Biochim. Biophys. Acta Bioenerg.* **1997**, *1322*, 86–105.
- (18) de Kerchove, A. J.; Elimelech, M. Bacterial swimming motility enhances cell deposition and surface coverage. *Environ. Sci. Technol.* **2008**, *42*, 4371–4377.
- (19) O'Toole, G. A.; Kolter, R. Flagellar and twitching motility are necessary for *Pseudomonas aeruginosa* biofilm development. *Mol. Microbiol.* **2002**, *30*, 295–304.
- (20) McClaine, J. W.; Ford, R. M. Characterizing the adhesion of motile and nonmotile *Escherichia coli* to a glass surface using a parallel-plate flow chamber. *Biotechnol. Bioeng.* **2002**, *78*, 179–189.
- (21) Herzberg, M.; Sweity, A.; Bami, M.; Kaufman, Y.; Freger, V.; Oron, G.; Belfer, S.; Kasher, R. Surface properties and reduced biofouling of graft-copolymers that possess oppositely charged groups. *Biomacromolecules* **2011**, *12*, 1169–1177.
- (22) Schofield, A. L.; Rudd, T. R.; Martin, D. Real-time monitoring of the development and stability of biofilms of *Streptococcus mutans* using the quartz crystal microbalance with dissipation monitoring. *Biosens. Bioelectron.* **2007**, *23*, 407–413.
- (23) Olsson, A. L. J.; van der Mei, H. C.; Busscher, H. J.; Sharma, P. K. Novel analysis of bacterium–substratum bond maturation measured using a Quartz Crystal Microbalance. *Langmuir* **2010**, *26*, 11113–11117.
- (24) Feiler, A. A.; Sahlholm, A.; Sandberg, T.; Caldwell, K. D. Adsorption and viscoelastic properties of fractionated mucin (BSM) and bovine serum albumin (BSA) studied with quartz crystal microbalance (QCM-D). *J. Colloid Interface Sci.* **2007**, *315*, 475–481.

- (25) Olsson, A. L. J.; Van Der Mei, H. C.; Busscher, H. J.; Sharma, P. K. Influence of Cell Surface appendages on the bacterium–substratum interface measured real-time using QCM-D. *Langmuir* **2008**, *25*, 1627–1632.
- (26) Poitras, C.; Fatisson, J.; Tufenkji, N. Real-time microgravimetric quantification of *Cryptosporidium parvum* in the presence of potential interferents. *Water Res.* **2009**, *43*, 2631–2638.
- (27) Olsson, A. L. J.; Van der Mei, H. C.; Busscher, H. J.; Sharma, P. K. Acoustic sensing of the bacterium–substratum interface using QCM-D and the influence of extracellular polymeric substances. *J. Colloid Interface Sci.* **2011**, *357*, 135–138.
- (28) Vanoyan, N.; Walker, S. L.; Gillor, O.; Herzberg, M. Reduced bacterial deposition and attachment by quorum-sensing inhibitor 4-nitro-pyridine-n-oxide: The role of physicochemical effects. *Langmuir* **2010**, *26*, 12089–12094.
- (29) Marcus, I. M.; Herzberg, M.; Walker, S. L.; Freger, V. *Pseudomonas aeruginosa* attachment on QCM-D sensors: The role of cell and surface hydrophobicities. *Langmuir* **2012**, *28*, 6396–6402.
- (30) De Kerchove, A. J.; Elimelech, M. Formation of polysaccharide gel layers in the presence of Ca²⁺ and K ions: Measurements and mechanisms. *Biomacromolecules* **2007**, *8*, 113–121.
- (31) Ying, W.; Yang, F.; Bick, A.; Oron, G.; Herzberg, M. Extracellular polymeric substances (EPS) in a hybrid growth membrane bioreactor (HG-MBR): Viscoelastic and adherence characteristics. *Environ. Sci. Technol.* **2010**, *44*, 8636–8643.
- (32) Bereschenko, L. A.; Prummel, H.; Euverink, G. J. W.; Stams, A. J. M.; van Loosdrecht, M. C. M. Effect of conventional chemical treatment on the microbial population in a biofouling layer of reverse osmosis systems. *Water Res.* **2010**, *45*, 405–416.
- (33) Bereschenko, L.; Heilig, G.; Nederlof, M.; van Loosdrecht, M.; Stams, A.; Euverink, G. Molecular characterization of the bacterial communities in the different compartments of a full-scale reverse-osmosis water purification plant. *Appl. Environ. Microbiol.* **2008**, *74*, 5297–5304.
- (34) Bereschenko, L.; Stams, A.; Euverink, G.; van Loosdrecht, M. Biofilm formation on reverse osmosis membranes is initiated and dominated by *Sphingomonas* spp. *Appl. Environ. Microbiol.* **2010**, *76*, 2623–2632.
- (35) Balkwill, D. L.; Fredrickson, J. K.; Rominem, M. F. *Sphingomonas* and related genera. In *The Prokaryotes: An Evolving Electronic Resource for the Microbiological Community*; Dworkin, M., et al., Eds.; Springer-Verlag: New York, 1999.
- (36) Pratt, L. A.; Kolter, R. Genetic analysis of *Escherichia coli* biofilm formation: Roles of flagella, motility, chemotaxis and type I pili. *Mol. Microbiol.* **1998**, *30*, 285–293.
- (37) Maniatis, T.; Fritsch, E. F.; Sambrook, J. *Molecular Cloning: A Laboratory Manual*; Cold Spring Harbor Laboratory Press: New York, 1989.
- (38) Pembrey, R. S.; Marshall, K. C.; Schneider, R. P. Cell surface analysis techniques: What do cell preparation protocols do to cell surface properties? *Appl. Environ. Microbiol.* **1999**, *65*, 2877–2894.
- (39) Sperandio, V.; Torres, A. G.; Kaper, J. B. Quorum sensing *Escherichia coli* regulators B and C (QseBC): A novel two-component regulatory system involved in the regulation of flagella and motility by quorum sensing in *E. coli*. *Mol. Microbiol.* **2002**, *43*, 809–821.
- (40) Chapman, D. L. A contribution to the theory of electro-capillarity. *Philos. Mag.* **1913**, *25*, 475–481.
- (41) Gouy, M. Sur la constitution de la charge electrique a la surface d'un electrolyte. *J. Phys. Theor. Appl.* **1910**, *9*, 457–468.
- (42) Gregory, J. *Particles in Water: Properties and Processes*; IWA Publishing: London, 2006.
- (43) Zhu, X.; Elimelech, M. Colloidal fouling of reverse osmosis membranes: Measurements and fouling mechanisms. *Environ. Sci. Technol.* **1997**, *31*, 3654–3662.
- (44) White, D. C.; Sutton, S. D.; Ringelberg, D. B. The genus *Sphingomonas*: Physiology and ecology. *Curr. Opin. Biotechnol.* **1996**, *7*, 301–306.
- (45) Kawasaki, S.; Moriguchi, R.; Sekiya, K.; Nakai, T.; Ono, E.; Kume, K.; Kawahara, K. The cell envelope structure of the lipopolysaccharide-lacking gram-negative bacterium *Sphingomonas paucimobilis*. *J. Bacteriol.* **1994**, *176*, 284–290.
- (46) Wiese, A.; Reiners, J. O.; Brandenburg, K.; Kawahara, K.; Zähringer, U.; Seydel, U. Planar asymmetric lipid bilayers of glycosphingolipid or lipopolysaccharide on one side and phospholipids on the other: Membrane potential, porin function, and complement activation. *Biophys. J.* **1996**, *70*, 321–329.
- (47) Lawrence, J. R.; Delaquis, P. J.; Korber, D. R.; Caldwell, D. E. Behavior of *Pseudomonas fluorescens* within the hydrodynamic boundary layers of surface microenvironments. *Microb. Ecol.* **1987**, *14*, 1–14.
- (48) Prigent-Combaret, C.; Vidal, O.; Dorel, C.; Lejeune, P. Abiotic surface sensing and biofilm-dependent regulation of gene expression in *Escherichia coli*. *J. Bacteriol.* **1999**, *181*, 5993–6002.
- (49) Sauer, K.; Camper, A. K. Characterization of phenotypic changes in *Pseudomonas putida* in response to surface-associated growth. *J. Bacteriol.* **2001**, *183*, 6579–6589.
- (50) Stanley, N. R.; Britton, R. A.; Grossman, A. D.; Lazazzera, B. A. Identification of catabolite repression as a physiological regulator of biofilm formation by *Bacillus subtilis* by use of DNA microarrays. *J. Bacteriol.* **2003**, *185*, 1951–1957.
- (51) Gibiansky, M. L.; Conrad, J. C.; Jin, F.; Gordon, V. D.; Motto, D. A.; Mathewson, M. A.; Stopka, W. G.; Zelasko, D. C.; Shrout, J. D.; Wong, G. C. L. Bacteria use type IV pili to walk upright and detach from surfaces. *Science* **2010**, *330*, 197.
- (52) Yonekura, K.; Maki-Yonekura, S.; Namba, K. Building the atomic model for the bacterial flagellar filament by electron cryomicroscopy and image analysis. *Structure* **2005**, *13*, 407–412.
- (53) Toutain, C. M.; Caizza, N. C.; Zegans, M. E.; O'Toole, G. A. Roles for flagellar stators in biofilm formation by *Pseudomonas aeruginosa*. *Res. Microbiol.* **2007**, *158*, 471–477.
- (54) Busscher, H. J.; Weerkamp, A. H. Specific and non-specific interactions in bacterial adhesion to solid substrata. *FEMS Microbiol. Lett.* **1987**, *46*, 165–173.